[15]K. Wirtz, Z. Physik 44, 221 (1943); and J. A. Brinkman, Phys. Rev. 93, 345 (1954).
[16]This method was used in Ref. 9 to calculate the fraction of the migration energy carried across the barrier by the jumping atom.
[17]H. B. Huntington, G. A. Shirn, and W. A. Wadja, Phys. Rev. 99, 1085 (1955).

PHYSICAL REVIEW B VOLUME 3, NUMBER 4 15 FEBRUARY 1971

Lattice Dynamics of Holmium†

R. M. Nicklow, N. Wakabayashi, and P. R. Vijayaraghavan*
Solid State Division, Oak Ridge National Laboratory, Oak Ridge, Tennessee 37830
(Received 28 October 1970)

The dispersion relation for the normal modes of vibration of holmium metal at room temperature has been measured by means of slow-neutron inelastic scattering techniques. Phonon frequencies for wave vectors along the principal symmetry directions have been determined and, in addition, some experimental information about the phonon frequencies along the boundaries of the Brillouin zone are reported. The data have been fitted with a Born–von Kármán force model which includes interactions out to the eighth nearest neighbor. The interactions have been assumed to be general (tensor) out to the fourth nearest neighbor and axially symmetric beyond. The model has been used to calculate a frequency distribution function $g(\nu)$, the lattice specific heat, and the corresponding Debye temperature.

I. INTRODUCTION

As part of a program to obtain detailed information about the lattice dynamics of the heavy rare-earth metals, we have made neutron inelastic scattering measurements of the phonon-dispersion relation of holmium at room temperature. Data have been obtained for all six branches of the dispersion relation in the principal symmetry directions. The data obtained along the zone boundaries are less complete than those obtained for Tb, but they are sufficient to permit the evaluation of the force-constant parameters in an eighth-nearest-neighbor model such as was used for Tb.[1] Previous measurements on Ho by Leake *et al.*[2] are in good agreement with our results where there is an overlap of the two sets of data.

The model fitted to the measured dispersion relation has been used to calculate a frequency distribution function for Ho, and this in turn has been used to calculate a variety of thermodynamic properties. In particular, the lattice specific heat has been calculated and compared with measurements[3] to permit the determination of the magnetic contribution to the total specific heat.

II. MEASUREMENTS AND RESULTS

The measurements were carried out at the Oak Ridge high-flux isotope reactor on a triple-axis neutron spectrometer. The majority of the data was obtained with the constant-Q method. For most of the measurements the analyzer was set to accept scattered neutrons with an energy E' corresponding to a frequency of 6 THz (~ 25 meV), although in order to check the data, some measurements were carried out using scattered neutrons with frequencies of 7.2 and 10 THz. As monochromator and analyzer the (0002) Bragg reflections from two Be crystals were used.

Two samples were studied. Both were irregularly shaped disks grown by the strain-anneal method by Reed of the Oak Ridge National Laboratory Solid State Division. One crystal, about 30 mm in diameter and 3 mm thick, was oriented with the c axis about 45° from the normal to the disk, and measurements in the ab plane were made with this crystal. The second sample, 20 mm in diameter and 6 mm thick, was oriented with the c axis nearly parallel to the normal of the disk, and was used for the remainder of the measurements. For Ho, the lattice parameters at room temperature are $a = 3.577$ and $c = 5.616$ Å.

A selection of measured phonon frequencies in Ho at room temperature is given in Table I, where they are compared to the corresponding frequencies in Tb.[1] The complete results are shown in Figs. 1 and

TABLE I. A selection of measured normal-mode frequencies in Ho and Tb at room temperature (10^{12} cps).

	Ho	Tb		Ho	Tb
Γ_6^-	1.94±0.03	1.82±0.03	Γ_3^+	3.40±0.07	3.25±0.04
A_3	1.34±0.03	1.30±0.02	A_1	2.56±0.04	2.44±0.04
M_4^-	1.96±0.03	1.75±0.03	M_4^+	1.65±0.03	1.59±0.04
			M_3^+	3.04±0.03	2.90±0.03
M_2^-	3.08±0.05	3.05±0.04	M_1^+	3.05±0.05	2.89±0.04
K_6	2.46±0.05	2.32±0.04			
$L_1(A)$	1.85±0.07	1.78±0.06			

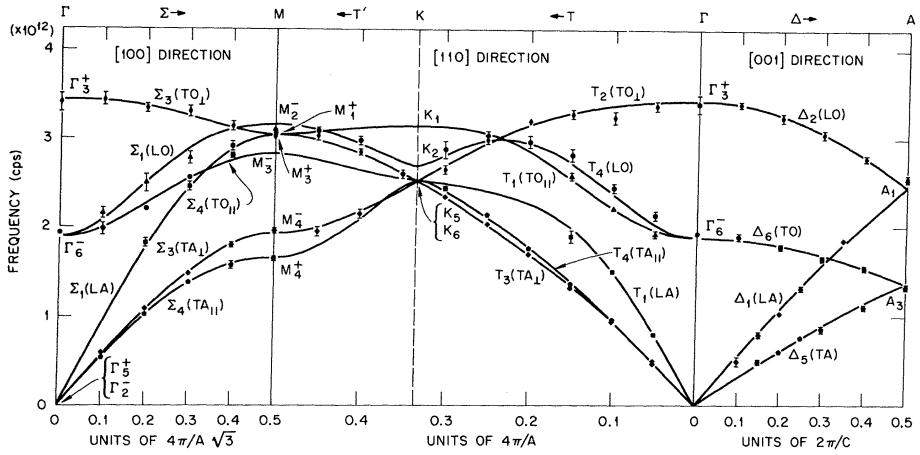

FIG. 1. Phonon dispersion curves for Ho in the major symmetry directions at room temperature. The lines shown represent the eighth-nearest-neighbor force model (see text).

2. The experimental errors are generally about 2%. Because of the high absorption cross section of holmium (80–100 b at the neutron energies used) and high incoherent-scattering cross section (~5 b), we were not able to obtain very much data along the boundaries of the Brillouin zone where the structure factors are generally low. Even for certain high-symmetry branches, mainly T_1, the data are sparse. The group-theoretical notation used by Raubenheimer and Gilat[4] has been followed. The solid curves are the result of a nonlinear least-squares fit to the data of a Born – von Kármán interatomic force model to be discussed in Sec. III.

All the experimental results given here were obtained with Soller-slit collimators [full width at half-maximum (FWHM) = 0.6°] both before and after the specimen. Where necessary, the data have been corrected for sloping background, but no other corrections have been applied.

III. THEORETICAL CALCULATIONS

A. Model

The data have been fitted with the Born – von Kármán atomic-force model that was used for Tb.[1] The model includes general (tensor) interactions out to the fourth nearest neighbors and axially symmetric interactions from the fifth to the eighth nearest neighbors. Since the dispersion relation measured for holmium is quite similar to that for terbium, we assumed that the force constants obtained for terbium would provide an adequate set of initial parameters for the nonlinear least-squares fitting of the holmium data. Thus, we did not perform the linear fitting carried out for Tb, nor did we investigate other types of models since more restrictive models were found inadequate for fitting the Tb data.[1] The solid lines in Figs. 1 and 2 show the fit obtained with this model, and in Table II are given

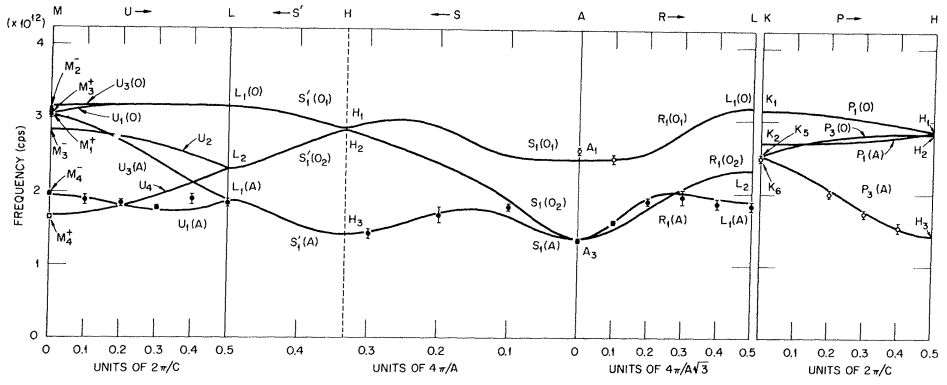

FIG. 2. Phonon dispersion curves for Ho along the boundaries of the Brillouin zone at room temperature. The lines shown represent the eighth-nearest-neighbor force model.

TABLE II. Best-fit eighth-nearest-neighbor force model for holmium.

Neighbor	Force constant	(dyn/cm)
1	α_1	7 054
	β_1	1 055
	γ_1	11 517
	δ_1	6 766
2	α_2	1 084
	β_2	12 716
	γ_2	- 927
	ϵ_2	2 259
3	α_3	- 1 496
	β_3	- 937
	γ_3	- 1 066
	δ_3	965
4	α_4	80
	γ_4	- 3 897
5	ϕ_r^5	488
	ϕ_t^5	- 11
6	ϕ_r^6	1 213
	ϕ_t^6	318
7	ϕ_r^7	1 048
	ϕ_t^7	- 133
8	ϕ_r^8	- 344
	ϕ_t^8	40

the values obtained for the force constants. The form of the force-constant matrices used here is the same as that described for Tb. Since the ϕ_t^7 parameter for Ho cannot be determined from the data presently available, we assumed that the ratio ϕ_t^7/ϕ_r^7 for Ho is the same as that determined for Tb.

TABLE III. Elastic constants for Ho calculated from eighth-neighbor model (10^{11} dyn/cm^2).

$C_{11} = 7.72$	$C_{44} = 2.75$
$C_{33} = 8.44$	$C_{66} = 2.62$

B. Calculations from Model

1. *Elastic Constants*

From the eighth-nearest-neighbor model we have calculated the elastic constants, and these are given in Table III. Good agreement exists between the longitudinal and shear velocity of sounds for the c direction obtained from these calculated elastic constants and those obtained experimentally.[5] Also, the elastic constants measured by Palmer[6] at 4 °K are consistent with these room-temperature values. The small differences (~ 3%) that exist between these two sets of constants are compatible with the usual effects of anharmonicity.

2. *Frequency Distribution Function*

This function has been computed using the method described by Raubenheimer and Gilat.[4] The result for Ho, obtained with the eighth-nearest-neighbor model, is shown in Fig. 3. This figure is an unsmoothed computer plot, with the histogram of

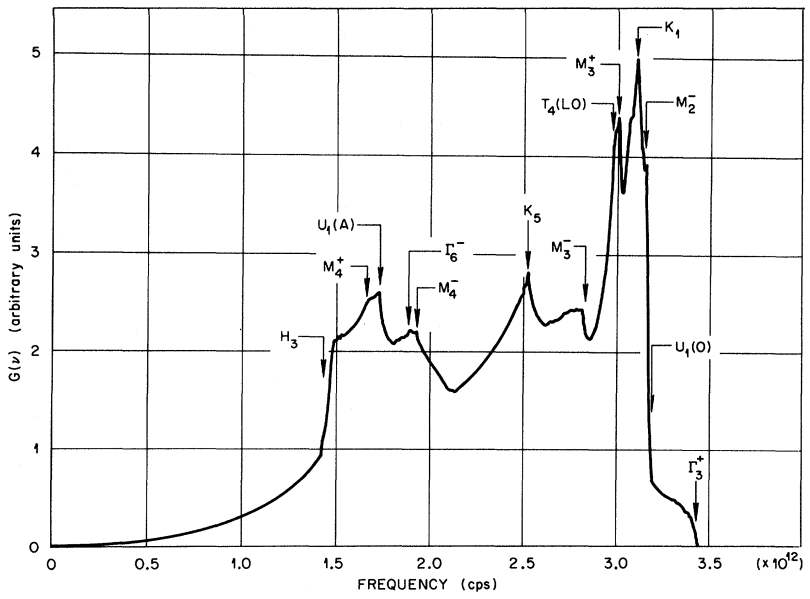

Holmium G(ν) from 8 Neighbor Model Fit to Inelastic Neutron Scattering Data.

FIG. 3. Phonon frequency distribution function for Ho. The critical point features which occur at the frequencies corresponding to the symmetry points of the dispersion curves in Figs. 1 and 2 are indicated.

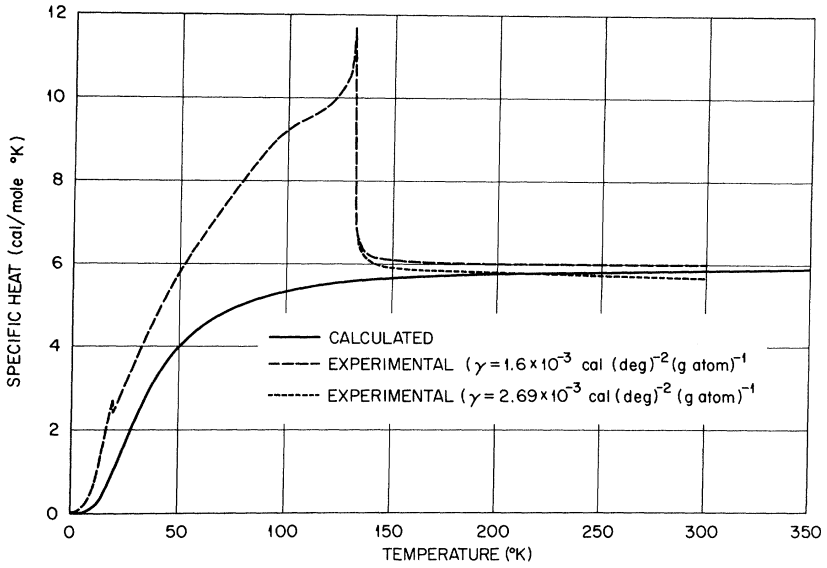

Specific Heat for Holmium.

FIG. 4. Comparison of the measured specific heat, corrected for electronic contributions, and the calculated lattice specific heat.

$g(\nu)\Delta\nu$ sorted into frequency channels of width $\Delta\nu = 0.0025$ THz. Critical points that can be identified from the calculated dispersion curves for the high-symmetry direction (see Figs. 1 and 2) are indicated. The frequency distribution function for Ho is naturally quite similar to that for Tb, but distinct differences exist. These differences are presumably related to the slightly different ordering of the frequencies at high-symmetry points (see Table I) in the two materials.

3. *Heat Capacity and Debye Temperature*

At low temperatures C_M, the magnetic contribution to the total specific heat C_P of Ho is large in comparison with the electronic (C_E), lattice (C_L), and nuclear (C_N) contributions. Recently, Lounasmaa and Sundström[7] have reported specific-heat measurements and analyses for many of the heavy rare-earth metals between 3 and 25 °K. In order to analyze the total specific heat into its components, they assumed that the lattice specific heats of all the magnetic rare-earth metals were the same as that measured for lutetium.

The lattice specific heat, however, may readily be computed in the harmonic approximation from the frequency distribution function $g(\nu)$. Using the $g(\nu)$ shown in Fig. 3, we have calculated C_L, the lattice specific heat of Ho, and the result of this calculation is shown in Fig. 4. In this figure we also show $C_P - C_E$. Since this quantity is equal to $C_M + C_L$, the area between the two curves shown in Fig. 3 is C_M (C_N can be neglected above 10 °K). In order to make a comparison between the measured and calculated specific heats up to room temperature, we have used C_P as that measured by Gerstein *et al.*[3] C_E has been calculated from $C_E = \gamma T$. Above about 130 °K the results we obtained using two different values for γ are indicated. The value of 2.69 cal/°K^2/*g* at. for γ is close to the average obtained from C_E measurements for the nonmagnetic rare-earth metals, which Lounasmaa and Sundström[7] suggested as a reasonable estimate of γ for the magnetic rare-earth metals. However, this γ is apparently too large for Ho since the resulting $C_P - C_E$ becomes smaller than the calculated C_L above 150 °K. At these temperatures, C_M is negligible and the calculated C_L is quite insensitive to the details of the calculated $g(\nu)$, so that the noted discrepancy could not be due to some inadequacy of the interatomic-force model which we obtained from the phonon-dispersion-relation measurements. It therefore appears quite possible that γ for Ho is nearer 1.6 cal/°K^2/g at., which is the value suggested by Gerstein *et al.*[3] A definitive examination of this problem would require an investigation of the (phonon) anharmonic contributions to C_P. On the other hand, one might expect γ to vary with temperature because of the temperature-dependent influence that the magnetic order may have on the electronic energy bands.[8,9]

The calculated $C_L + C_E$ for Ho, using either value for γ mentioned above, is in fair agreement ($\pm 10\%$) with the measurements for lutetium.[10,11] Thus, the conclusions of Lounasmaa and Sundström[7] concerning the temperature dependence of C_M below 10 °K for Ho probably would not be significantly altered if one were to analyze the C_M obtained from C_P data and the C_L calculations displayed in Fig. 4.

The calculated Debye temperature Θ is shown in Fig. 5. For comparison we show also the Debye temperatures obtained from low-temperature elas-

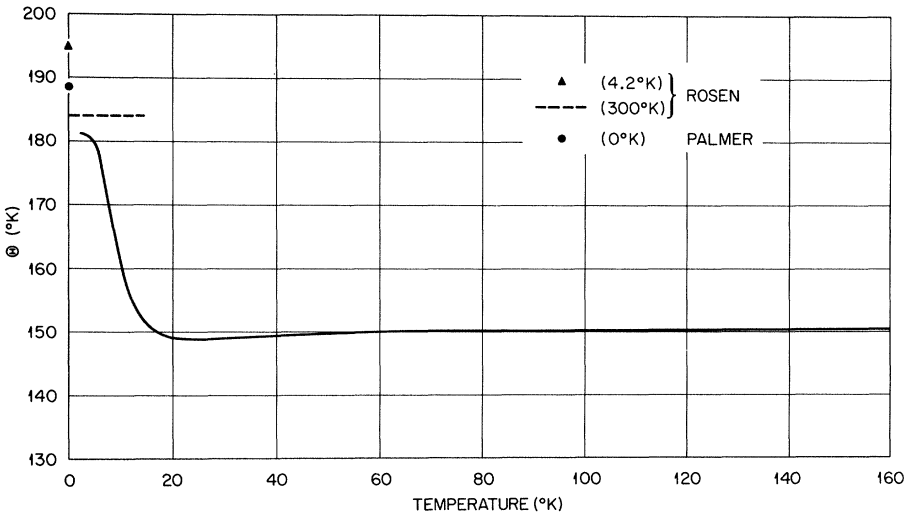

FIG. 5. Temperature dependence of the Debye temperature, derived from the calculated lattice specific heat. The various experimental values were obtained from elastic-constant measurements (Refs. 6 and 12).

Debye Temperature for Holmium.

tic-constant measurements made by Palmer[6] on single crystals and by Rosen[12] on polycrystalline samples. The measurements of Palmer are nearer our calculations. Actually, since the calculated curve is based on a $g(\nu)$ appropriate to ~300 °K, a correction for anharmonic effects should be applied before making such a comparison with low-temperature measurements. The magnitude of such a correction at 4 °K is probably close to the difference between the high- and low-temperature measurements of Rosen shown in Fig. 5.

IV. DISCUSSION

The plasma frequency ν_P, given by $\nu_P^2 = e^2 Z_n^2/\pi m$, where Z is the valence, m is the atomic mass, and n is the number of atoms per unit volume, is sometimes used as a normalizing frequency for comparing the dynamical properties of different metals. If the dynamics of Tb and Ho could be described by Coulomb interactions between positive ions embedded in a uniform negative charge, the normalized frequencies for these metals would be equal, or since ν_P is the same for Ho and Tb, the measured frequency would be equal. However, as illustrated in Table I, the phonon frequencies for Ho are approximately 5% higher than those for Tb. Thus, although the dispersion relation for Ho is qualitatively very similar to that for Tb, significant differences exist which are perhaps related to differences in the electronic structure and hence the interatomic forces of these two materials and not to the small differences in atomic mass and volume. It is expected that a systematic study of the dynamical properties of all the rare-earth metals eventually may be correlated to a systematic study of their electronic structure.

One aspect of the comparison between Ho and Tb is at present a little puzzling. Ho possesses a spiral magnetic structure over a much wider temperature range than does Tb. Since this type of magnetic order can be related to the existence of parallel sheets of the Fermi surface which are separated by $\vec{k}_0$, the wave vector of this spiral,[9] it was anticipated that an easily detectable Kohn-type anomaly might exist in the phonon spectrum of Ho for $\vec{q} = \vec{k}_0$, even though very little evidence of one was found for Tb.[1] This was not the case; only very little evidence of such an anomaly was also found for Ho. However, there may be anomalies at other wave vectors that were overlooked, and a search will be made for them in the future. In any event, all such anomalies in Ho must be very small.

V. SUMMARY

Neutron inelastic scattering measurements of the phonon-dispersion relation of holmium have been analyzed by means of an eighth-nearest-neighbor Born – von Kármán force model which includes tensor interactions for the first four nearest neighbor shells. The model obtained from this analysis has provided the basis for a calculation of a frequency distribution function for Ho and this in turn has been used to calculate the lattice specific heat and the corresponding Debye temperature as a function of temperature.

A comparison of these data with similar data recently reported for Tb[1] indicates that although the phonon dispersion relations for Ho and Tb are qualitatively very similar, significant differences exist which are presumably related to differences in their electronic structure. On the other hand, the differences in the electronic structure which are respon-

sible for giving Ho a stronger tendency toward a spiral magnetic order do not result in a measurably larger Kohn-type anomaly in the phonon spectrum of Ho.

†Research sponsored by the U.S. Atomic Energy Commission under contract with the Union Carbide Corporation.

*Present address: Bhabha Atomic Energy Research Centre, Trombay, Bombay, India.

[1]J. C. Gylden Houmann and R. M. Nicklow, Phys. Rev. B 1, 3943 (1970).

[2]J. A. Leake, V. J. Minkiewicz, and G. Shirane, Solid State Commun. 7, 535 (1969).

[3]B. C. Gerstein, M. Griffel, L. D. Jennings, R. E. Miller, R. E. Skochdopole, and F. H. Spedding, J. Chem. Phys. 27, 394 (1957).

[4]L. J. Raubenheimer and G. Gilat, Phys. Rev. 157, 586 (1967).

[5]R. J. Pollina and B. Luthi, Phys. Rev. 177, 841 (1969).

[6]S. B. Palmer, J. Phys. Chem. Solids 31, 143 (1970).

[7]O. V. Lounasmaa and L. J. Sundström, Phys. Rev. 150, 399 (1966); 158, 591 (1967).

[8]R. J. Elliott and F. A. Wedgwood, Proc. Soc. (London) 81, 846 (1963).

[9]W. E. Evenson and S. H. Liu, Phys. Rev. 178, 783 (1969).

[10]B. C. Gerstein, W. A. Taylor, W. D. Shickell, and F. H. Spedding, Phys. Rev. 51, 2924 (1969).

[11]H. V. Culbert, Phys. Rev. 156, 701 (1967).

[12]M. Rosen, Phys. Rev. Letters 19, 695 (1967).

PHYSICAL REVIEW B VOLUME 3, NUMBER 4 15 FEBRUARY 1971

Study of the Martensitic Phase Transition in Sodium†

Galen K. Straub* and Duane C. Wallace
Sandia Laboratories, Albuquerque, New Mexico 87115

(Received 9 July 1970)

The martensitic transformation in sodium is studied by means of a local pseudopotential theory. The total Helmholtz free energy is calculated as a function of temperature and crystal configuration for both the bcc and hcp phases of sodium. At $T=0$, the hcp phase is found to be stable, while the bcc phase is found to be stable at high temperatures. The inclusion of the zero-point energy at $T=0$ gives improved agreement with the experimentally determined energy differences between the bcc and hcp phases. It is found that the thermal expansion of the crystal does not play a significant role in the phase transition and the transition from hcp to bcc as the temperature increases can be explained by thermodynamic arguments.

I. INTRODUCTION

A martensitic phase transition has been observed in sodium around 36 °K.[1] As the temperature is lowered, the high-temperature bcc structure changes to a close-packed hexagonal structure (non-ideal ratio). In order to study this transition, we have used a simple local pseudopotential model to calculate the Helmholtz free energy for both the bcc and hcp structures. Previous calculations[2,3] to determine the stable crystal structure of sodium have calculated the band structure and electrostatic energies at $T=0$ of the bcc and hcp phases at fixed volume. In the present calculation, the total free energy as a function of the crystal configuration is calculated and then minimized at each temperature with respect to the configuration. Our calculations show an energy difference at $T=0$ that is approximately twice the experimentally determined energy difference, and the total free energy predicts a phase transition from the cubic to hexagonal structure at a transition temperature about seven times the observed transition temperature.

In Sec. II the local pseudopotential used in this calculation is briefly described, and in Sec. III the calculation of the total free energy is described with emphasis on the hexagonal free energy and the procedure used to minimize it. In Sec. IV we discuss the relative importance of volume-dependent vs structural-dependent terms in the free energy, and give thermodynamic arguments for the explanation of the cubic to hexagonal transition.

II. DESCRIPTION OF LOCAL PSEUDOPOTENTIAL

One of the features of pseudopotential theory is that the pseudopotential can be separated into terms that are structure dependent and terms that are dependent only upon the total crystal volume. Thus, one is able to compare different crystal structures and, as in this case, specifically incorporate the structural differences in the calculation of the total Helmholtz free energy.

Because of its analytical simplicity, we have chosen Harrison's modified point-ion pseudopotential and included a Born-Mayer repulsion between ion cores. The pseudopotential contains two ad-